



First and second vacuum-PVD improvement of soft Bangkok clay for the third runway of Suvarnabhumi International Airport Thailand

Dennes T. Bergado¹ · Pitthaya Jamsawang² · Panich Voottipruex³ · Pornkasem Jongpradist⁴ · Jansen Rementilla¹ · Sjors Dicker⁵

Received: 3 March 2024 / Accepted: 20 June 2024 / Published online: 16 August 2024
© Springer Nature Switzerland AG 2024

Abstract

This paper applies a modified vacuum-PVD system combined with the embankment surcharge and multiple field distributed air-water separation sub-tanks to improve soft Bangkok clay. The system efficiently generated and maintained vacuum pressures from -80 to -90 kPa at the top of the embankment surcharge. The case study involved the construction of the third runway of Suvarnabhumi International Airport Thailand, which was built on soft Bangkok clay deposits. The back-calculation results of monitored data from the second improvement of the third runway extension were compared with the corresponding results of the first improvement of the taxiway extension, including the evolutions of settlements, excess pore pressures, and flow parameters. The second improvement with 29 kPa surcharge had lower settlements but recorded higher pore pressures and flow parameters. The first improvement with 34 kPa surcharge registered higher settlements but indicated lower pore pressures and flow parameters. The unit weights, water contents, liquid limits, compression indices, and void ratios were reduced. The undrained shear strengths, maximum past pressures, and over-consolidation ratio were increased. Inward lateral movements perpendicular to the surcharge embankment due to higher vacuum pressures than the lower embankment surcharge load were observed. The surcharge embankment combined with the modified vacuum-PVD system using an airtight membrane and horizontal prefabricated drain has been successfully applied to improve soft Bangkok clay.

Keywords Consolidation · Ground improvement · Settlement · Soft Bangkok clay · Vertical drain

Introduction

Prefabricated vertical drain (PVD) is the cheapest and most widely applied method of soft ground improvement [1,2]. PVDs are artificial drainage paths installed vertically on soft

ground. This technique involves shortening the drainage path and taking advantage of the higher horizontal permeability in the soft ground deposit. The hydraulic gradient due to the preloading generates a horizontal pore water flow into the PVDs. Then, the pore water can flow vertically along

✉ Pitthaya Jamsawang
pitthaya.j@eng.kmutnb.ac.th

Dennes T. Bergado
bergado@ait.asia

Panich Voottipruex
pnv@kmutnb.ac.th

Pornkasem Jongpradist
pornkasem.jon@kmutt.ac.th

Jansen Rementilla
st121264@ait.ac.th

Sjors Dicker
sjors.dicker@boskalis.com

¹ Asian Institute of Technology, Pathum Thani
12120, Thailand

² Soil Engineering Research Center, Department of Civil Engineering, King Mongkut's University of Technology North Bangkok, Bangkok, Thailand

³ Department of Teacher Training in Civil Engineering, King Mongkut's University of Technology North Bangkok, Bangkok, Thailand

⁴ Construction Innovations and Future Infrastructures Research Center, Department of Civil Engineering, Faculty of Engineering, King Mongkut's University of Technology Thonburi, Bangkok 10140, Thailand

⁵ Boskalis, Papendrecht, Netherlands

the drain toward the permeable drainage layers. However, the PVD installation using a mandrel causes disturbances or smears in the clay surrounding the PVD, resulting in lower horizontal permeability in the smear zone [1, 3]. PVDs with embankment preloading combined with vacuum pressure (called vacuum PVD) have minimized the instability problem and accelerated the consolidation rate. Kjellman [4] first proposed vacuum consolidation in the early 1950s. Subsequently, the studies of vacuum consolidation continued up to the present [5–14].

Vacuum preloading can reduce the pore pressure and maintain constant total stress instead of increasing it because it utilizes atmospheric pressure as a surcharge load to accelerate soil consolidation. Preloading using PVDs with and without vacuum pumping is Southeast Asia's most popular soft ground improvement method. The improvement method has been well developed over the years because of intensive research and field applications [7, 13–18], including clogging effects [19,20] and booster [21]. A disadvantage of using only vacuum preloading with PVD is that it may cause large cracks in the surrounding area due to inward lateral displacements of the ground induced by the vacuum pressures. In contrast, surcharge embankment preloading can induce outward lateral displacements. Thus, the combined vacuum PVD and surcharge embankment method can control the magnitude of lateral displacements.

Vacuum preloading combined with surcharge embankment and PVDs can consist of drainage systems, sealing systems, and vacuum pumps. Vacuum pressures generated at the vacuum pumps spread into the underlying soft clays along the drainage system, sucking out water and accelerating consolidation. The drainage system consists of an interconnected network of PVDs, horizontal drains, sand layers, and perforated pipes, forming a complete path for spreading the vacuum pressures and facilitating the water drainage.

The sealing system consists of geomembranes protected by geotextiles to create an airtight isolation system. The main advantages of preloading with vacuum pumping are lower surcharge, lesser lateral displacement, no need for a smaller counterweight berm, and shorter construction time. There are several methods for applying vacuum pressure to soft ground, such as using direct tubing, membrane and sand blanket, membrane and horizontal prefabricated drains, and membrane and flexible perforated tube. Long et al. [12] discussed these methods in detail. Bergado et al. [13] recently conducted a successful case study with a numerical simulation of vacuum PVD combined with surcharge preloading using a modified air-water separation system. The air-water separation pump separates the water from the air that is sucked together from underground. The air is connected to the vacuum pump, and the water is pumped out by a submersible pump at the base of the air-water separation pump.

Construction site location, subsurface investigation, and vacuum-PVD system

The construction site was located in Samut Prakan province, approximately 30 km southeast of Bangkok, at the Second Bangkok International Airport, now known as Suvarnabhumi International Airport, in the central plain of Thailand, with an area of 8 by 4 km (Fig. 1a and b). The present operating runways consist of the first and second runways. This project site was divided into different zones for the airport expansion into the third runway. This case study was concerned mainly with zones 5, 7, 25, and 27 (Fig. 2). Zones 5 and 7 were located in the third runway extension (North), which was partially improved (first improvement) using the conventional PVD method with 5 m embankment surcharge and 10 m length of PVD during the years 2005 to 2007. The



Fig. 1 Locations of (a) Samut Prakan province, Thailand, and (b) Construction site at Suvarnabhumi International Airport

Fig. 2 Locations of zones 5 and 7 and zones 25 and 27 and corresponding bore holes in the third runway extension (North) and taxiway D extension, respectively



second improvement of the third runway extension (North) was necessary to increase the maximum past pressure to at least 120 kPa. Zones 25 and 27 within taxiway extension D were located in an unimproved area of soft Bangkok clay (Fig. 2). The first improvement of the taxiway extension D and the second improvement of the third runway extension (north) of the Suvarnabhumi International Airport used vacuum-PVD method combined with surcharge embankment as well as airtight membrane system, modified air-water separation tanks, and horizontal drains.

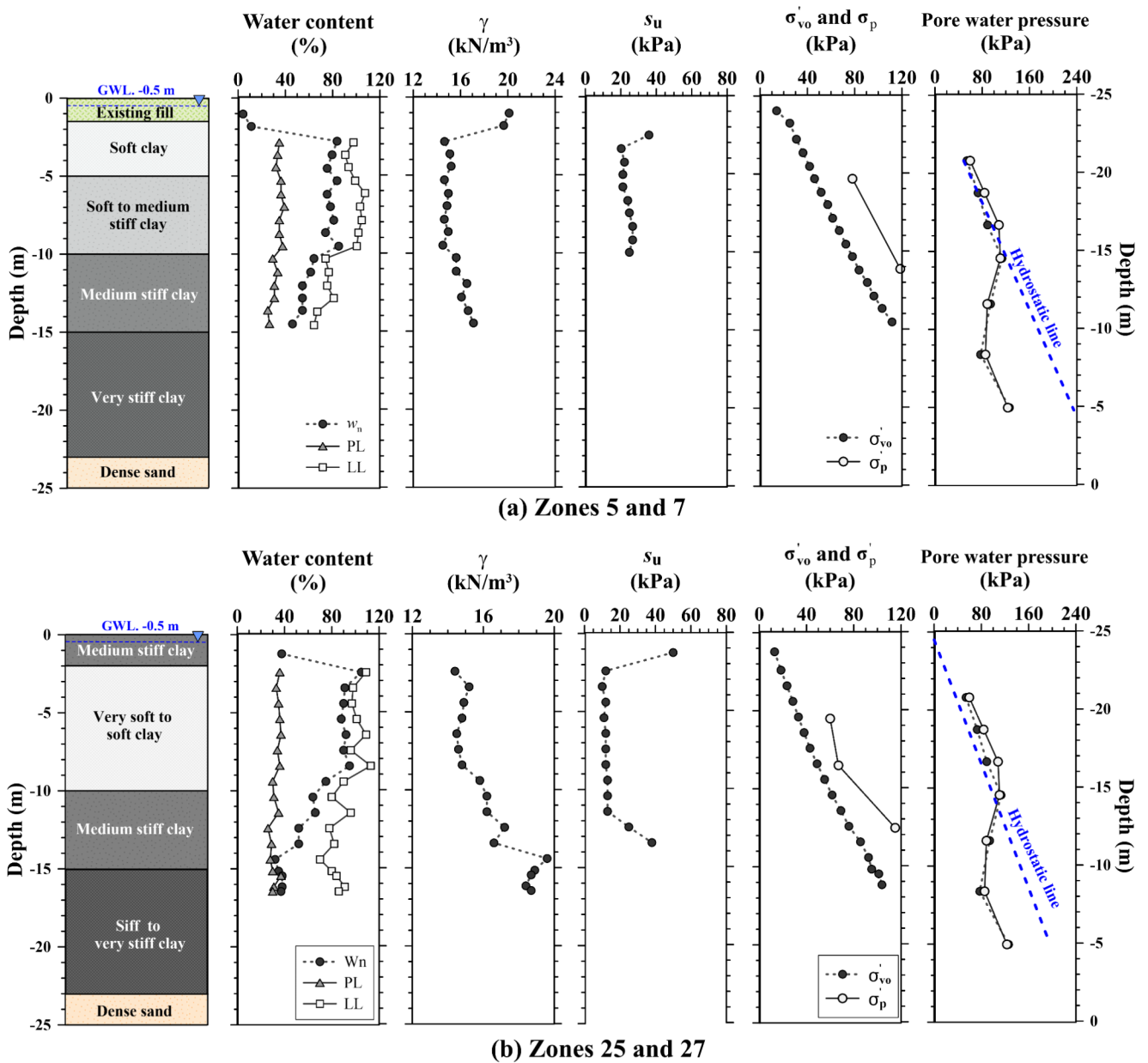
Figure 3a and b show the soil profiles of this case study in zones 5 and 7, as well as 25 and 27, respectively. Geotechnical investigations consisted of boreholes BH-02, BH-08, and BH-09, as well as field vane tests (FVT-4 and FVT-5) for zones 5 and 7 in the third runway extension as shown in Fig. 3a. The sand blanket and crushed rock from the first improvement was excavated to the original ground level before placement of the new surcharge fill and PVD installation for the second improvement. The new surcharge fill consisted of a 0.5-m-thick sand blanket and 1.0-m-thick crushed rock. Figure 4a demonstrates the simplified soil profile of zones 5 and 7, indicating an uppermost layer of 1.5-m-thick new surcharge fill materials underlain by 14-m-thick soft to medium clay followed by very stiff to hard clay layer and dense to very dense sand layer. A summary of soil physical and compressibility properties is tabulated in Table 1. After the first and partial improvement in zones 5 and 7, the soil profile and properties are also plotted in Fig. 3a, with the piezometric drawdown starting at 12 m depth due to groundwater extraction from the underlying sand layers for water supply. Vacuum preloading water extraction is only done from a shallow soft clay layer. After the second improvement, the soil properties were obtained from boreholes BH-1 and BH-2 and the field vane test (FVT-1) and compared for verification.

From boreholes BH-06, BH-22, and BH-24, as well as field vane test (FVT-16) for zones 25 and 27 in the unimproved area of the taxiway extension D, the simplified soil

profile consisting of the topmost 2-m-thick weathered clay layer underlain by 14-m-thick of very soft to soft clay followed by stiff to very stiff clay layer and dense to very dense sand layer as shown in Fig. 4b. The summary of the soil properties was tabulated in Table 2. A similar piezometric drawdown is also observed in this area, as shown in Fig. 4a.

Field monitoring instrumentations

The instrumentation plan layout is given in Fig. 5 for zones 5, 7, 25, and 27, consisting of surface settlement plates, pushed-in, bored piezometers, extensometers, and inclinometers. The instrumentation arrangements, with depth for zones 5, 7, 25, and 27, are shown in Fig. 6. The surface settlement plate was made of a 16-mm-diameter riser steel rod welded to a square-base steel plate with a size of 0.4 × 0.4 m and thickness of 3 mm. Optical leveling measurements to the top of the riser provide a record of plate elevations. Two types of GEOCON piezometers were utilized to monitor pore water pressure induced by the vacuum pressures: pushed-in and bored piezometers. The model 4500DP pushed-in piezometer has the transducer inside a housing with a drill rod thread and removable pointed nose cone. The model 4500 bored standard piezometer was designed to measure fluid pressures such as groundwater elevations and pore pressures when installed inside boreholes and observation wells. The pushed-in and bored piezometers monitored the pore water pressures at -5 m and -10 m elevations in the middle and bottom of the improved soft clay layer. The GEOCON digital inclinometer system was used to monitor the lateral displacement profiles of the improved ground during the vacuum and surcharge preloading with PVD. The system includes a 6100D digital inclinometer probe, a reel-mounted cable, and a readout data logger. The inclinometer casing used in this project was a 65-mm-diameter plastic pipe. Based on the practical work, the inclinometer casings



Remark

s_u = Undrained shear strength obtained from field vane shear test, σ'_{vo} = Effective overburden stress, σ'_p = Preconsolidation pressure

Fig. 3 Soil profiles of this case study

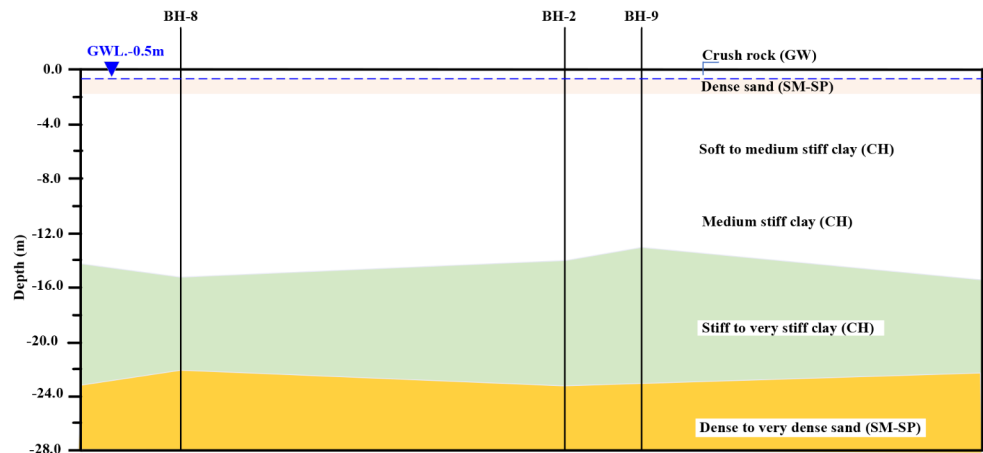
were installed up to the stiff clay layer at -18 m, sufficient to obtain a zero reading at this depth.

Modified vacuum-PVD system and improvement procedure

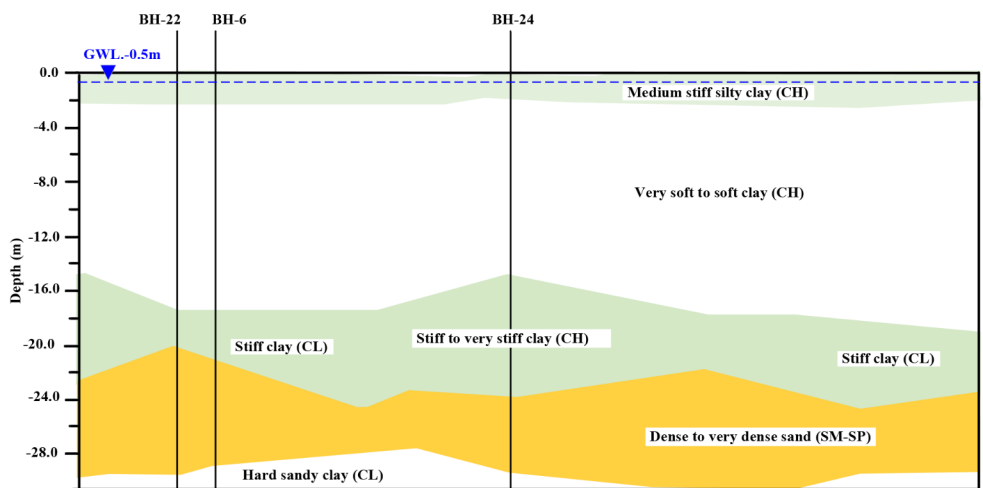
The soft ground improvement using vacuum-PVD with airtight membranes consisted of installed PVDs connected to the horizontal drains. It wrapped perforated pipes (wrapped around with non-woven geotextiles) within the sand blanket

to the vacuum pump at the ground surface to accelerate the consolidation process. The layout and pattern of the installations are indicated in Fig. 7. The 10-m-long PVDs with 1.0 m spacing in the square pattern were installed from the 0.5 m thick sand drainage blanket (equivalent to 9 kPa surcharge) through 1.5 m existing fill to -10 m elevation. The typical cross-section of the new vacuum-PVD system with a field-distributed air-water separation system is shown in Fig. 7. The PVDs were attached to the horizontal strip drains located within the 0.5 m thick sand blanket. The vacuum

Fig. 4 Simplified soil profiles of this case study



(a) Zones 5 and 7



(b) Zones 25 and 27

Table 1 Soil properties after the first improvement using PVD with embankment surcharge for zones 5 and 7 obtained from BH-02, BH-08, and BH-09

Properties	Symbol	Unit	Depth (m)				
			0.0 to -0.5	-0.5 to -1.5	-1.5 to -10.0	-10.0 to -15.0	-15.0 to -23.0
			Crushed rock	Sand blanket	Soft to medium stiff clay	Medium stiff clay	Stiff to very stiff clay
Soil classification			GW	SM-SP	CH	CH	CL
Unit weight (kN/m ³)	γ	kN/m ³	21	18	15–16	16–17	19
Natural water content (%)	w_n	%	8	10	82.5	75	40
Liquid limit, LL (%)	LL	%			74–106	65–80	
Plastic index, PI (%)	PL	%			44–69	39–50	
Pre-consolidation pressure	σ'_c	kPa			78–118	100–110	300
Initial void ratio	e_o				2.233	1.723	
Compression ratio	CR				0.26–0.35	0.26–0.29	0.16
Recompression ratio	RR				0.028–0.034	0.018–0.041	0.018
Vertical consolidation coefficient	c_v	m ² /yr			2–3	3	5
Horizontal permeability	k	m/yr	Permeable	Permeable	0.024	0.059	0.025

Table 2 Soil properties for zones 25 and 27 from BH-06, BH-22 and BH-24

Properties	Symbol	Unit	Depth (m)			
			0.0 to -2.0	-2.0 to -10.0	-10.0 to -15.0	-15.0 to -23.0
			Medium stiff clay	Very soft to soft clay	Medium stiff clay	Stiff to very stiff clay
Soil classification			CH	CH	CH	CL
Unit weight (kN/m ³)	γ	kN/m ³	17.5	15–16	16–17	18–19
Water content (%)	w	%	38–46	75–105	52–68	34–38
Liquid limit, LL (%)	LL	%		90–113	78–96	70–91
Plastic index, PI (%)	PL	%		60–77	49–60	42–60
Pre-consolidation pressure	σ'_p	kPa	60	60–67	115–150	300
Initial void ratio	e_o	-		2.58	1.54	-
Compression ratio	CR		0.33	0.33–0.37	0.26–0.30	0.15
Recompression ratio	RR		0.05	0.051	0.015–0.034	0.015
Vertical consolidation coefficient	c_v	m ² /yr	1	1	2.25	3.75
Horizontal permeability	k	m/yr	0.022	0.015	0.044	0.018

pressures were consistently generated by vacuum pumps and efficiently assisted by the field-distributed air-water separation tank. The sealing layer HDPE geomembrane was laid out on the sand blanket. Three layers of geotextiles were also installed below and above the geomembrane as protection against puncture and below the sand blanket as a separation layer. The horizontal strip drains were connected to the wrapped perforated pipes and the vacuum pump. The pore water discharges can be observed. An additional 1.0 m thick surcharge fill equivalent to 20 kPa was added on top of the sand blanket after the completion of the PVD connections.

The modified air-water separation system (Figs. 7 and 8) utilized multiple air-water separations in the field connected to a large vacuum pump station. By separating the air and water at various locations in the field using subtanks (Fig. 8) with submersible water pumps, the turbulent flow can be minimized in all the water conduits, strip drains, collector pipes, and mainly all the hoses running to the pumps to generate high-efficiency vacuum-PVD system. The large vacuum pump station (Fig. 8) covers a 30,000 m² improvement area. The vacuum pumps can reach incredibly high levels using an oil-lubricated rotary vane system with increased vacuum capacity. The pumps consisted of a large backup air-water separation system with tandem water tanks so the water could be pumped out while the other tanks were being filled. The vacuum pumps are computer-controlled to optimize energy consumption while maintaining the desired vacuum levels by switching between the five individual vacuum pumps inside the unit. Each 2,500 m² sub-area was fitted with a large meter and a field-distributed vacuum pump sub-tank assembly (Fig. 8) to monitor vacuum pressure and maintain efficiency. To pump out water, submersible pumps with a power of 1.0 kW were used at each sub-tank assembly to provide maximum vacuum efficiency.

Surcharge load and vacuum pressure loading

The surcharges consisted of a construction platform and sand blanket where the horizontal drains and perforated pipes to the vacuum pump were located. The surcharge loads used for the first improvement areas (zones 25 and 27) slightly differed from the second improvement areas (zones 5 and 7). A 0.8-m-surcharge fill (16 kPa) on top of a 1.0-m-thick sand blanket (18 kPa) was used for the first improvement areas; meanwhile, a 1.0-m-high surcharge fill (20 kPa) on top of the 0.5-m-thick sand blanket (9 kPa) was used for the second improvement areas. Furthermore, the second improvement area also had an existing sand blanket and crushed rock fill from the previous first improvement after cutting to the original ground surface. Vacuum pressures of approximately -80 to -90 kPa were successfully produced at the sand blanket under the HPDE geomembrane. However, the surcharge pressures were small compared to the vacuum pressures; they affected the settlement values of the improved soft clay and were used in settlement calculation [13]. Vacuum pressures of approximately -80 to -90 kPa were successfully produced at the sand blanket under the HPDE geomembrane. They were maintained effectively using field-distributed air-water separation tanks, and a combined loading of surcharge fill and vacuum was applied to all four zones. Vacuum pumping commenced in May 2021 for the second improvement areas, while pumping began in January to March 2022 for the first improvement areas. After 183 to 222 days, vacuum pumping was terminated for each location, and surcharge fill was compacted to be used as runway pavements. Figure 8 shows photos of the vacuum-PVD system used in the case study.

Fig. 5 Instrumentation plan for Zones 5, 7, 25 and 27

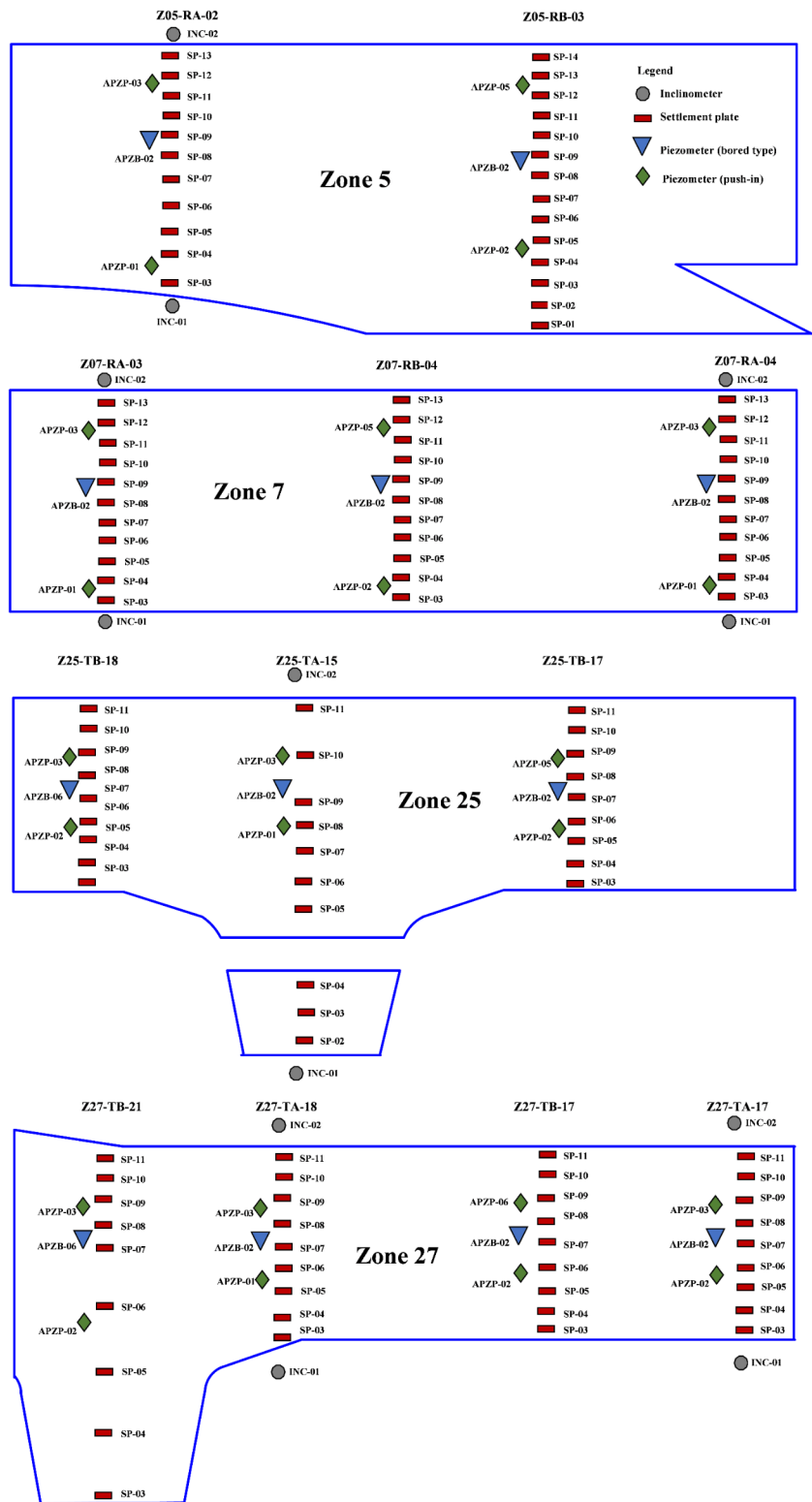


Fig. 6 Similar instrumentations for field monitoring in Zones 5, 7, 25, and 27

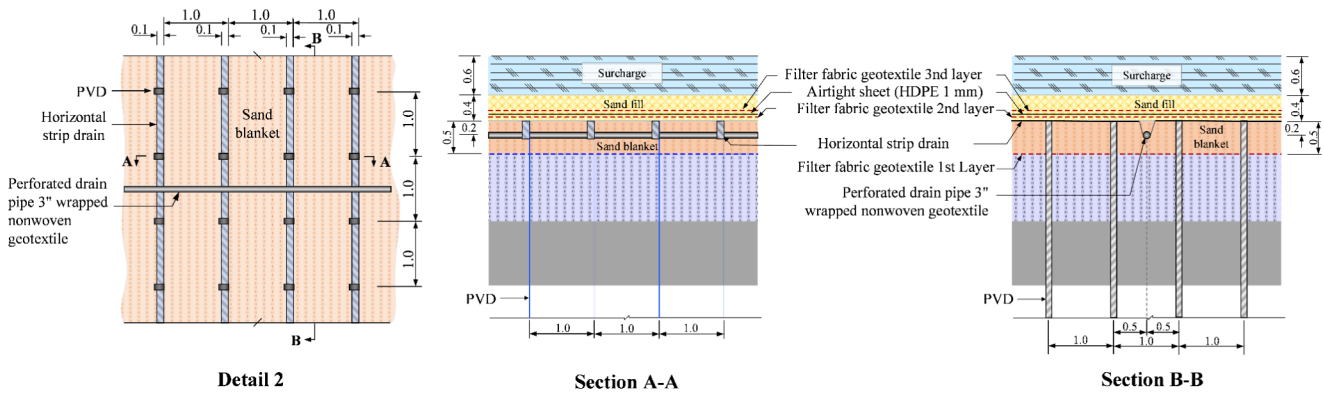
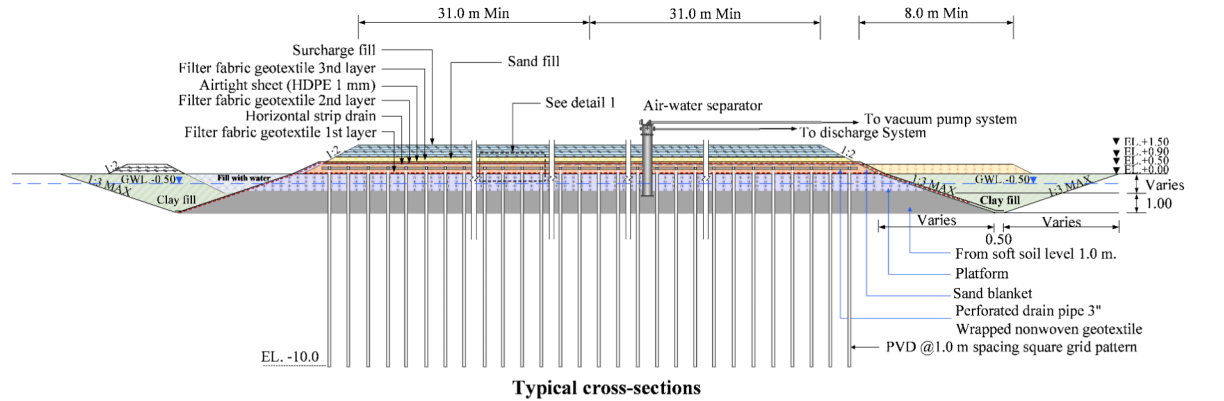
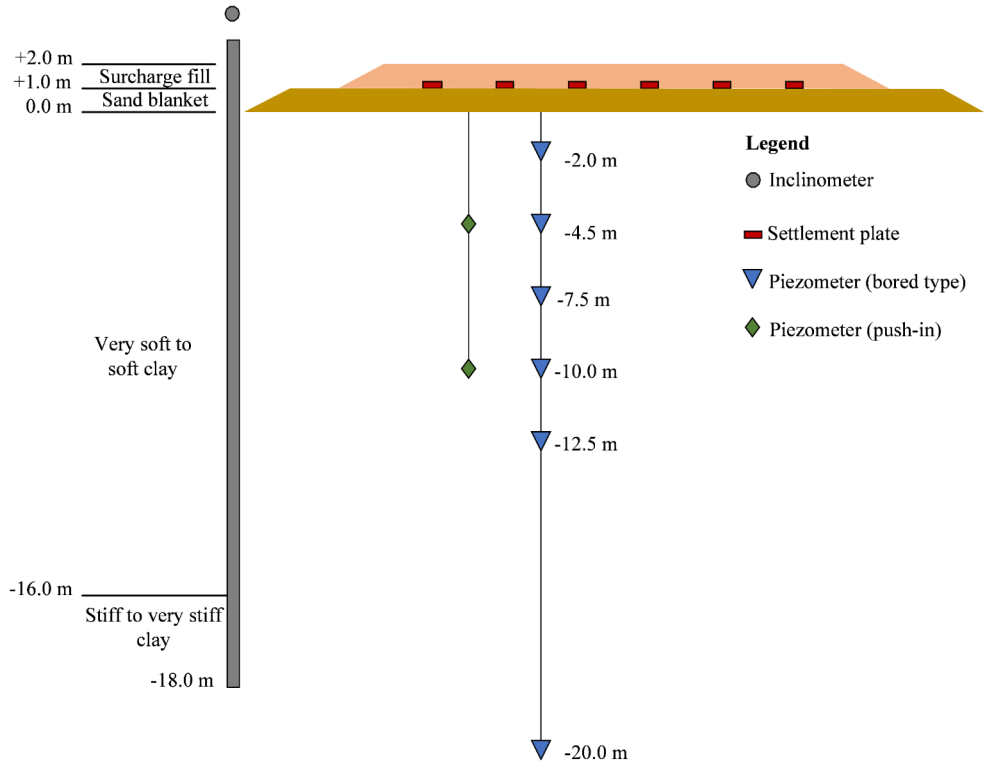


Fig. 7 Details of vacuum-PVD system for zones 5, 7, 25, and 27

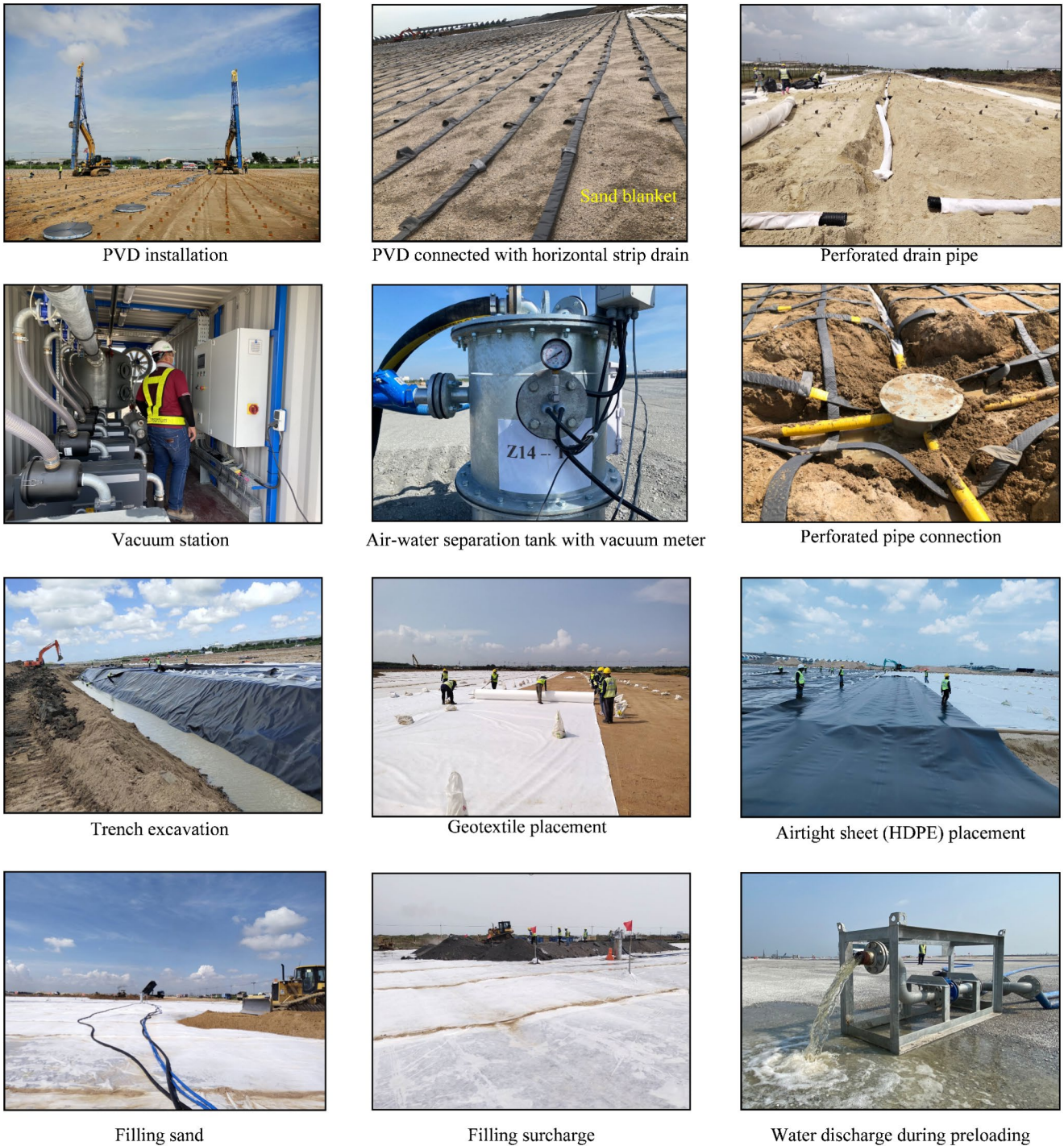


Fig. 8 Actual photos of the vacuum-PVD system

Data analyses

Surface settlements and rate of settlements with time

The vertical settlements were monitored using 113 surface settlement plates installed inside the improvement areas. As shown in Fig. 5, zones 5, 7, 25, and 27 have

25, 33, 28, and 27 settlement plates in RA, RB, TA, and TB, respectively. The magnitudes and rates of measured settlements with time are shown in Fig. 9, where the difference in magnitudes can be clearly distinguished. The settlement measurements ended at a 90% degree of consolidation with a corresponding rate of settlements of less than 5 mm per day [12, 22]. As expected, the settlements

Fig. 9 (a) Vacuum and surcharge (b) surface and (c) rate of settlements versus elapsed time

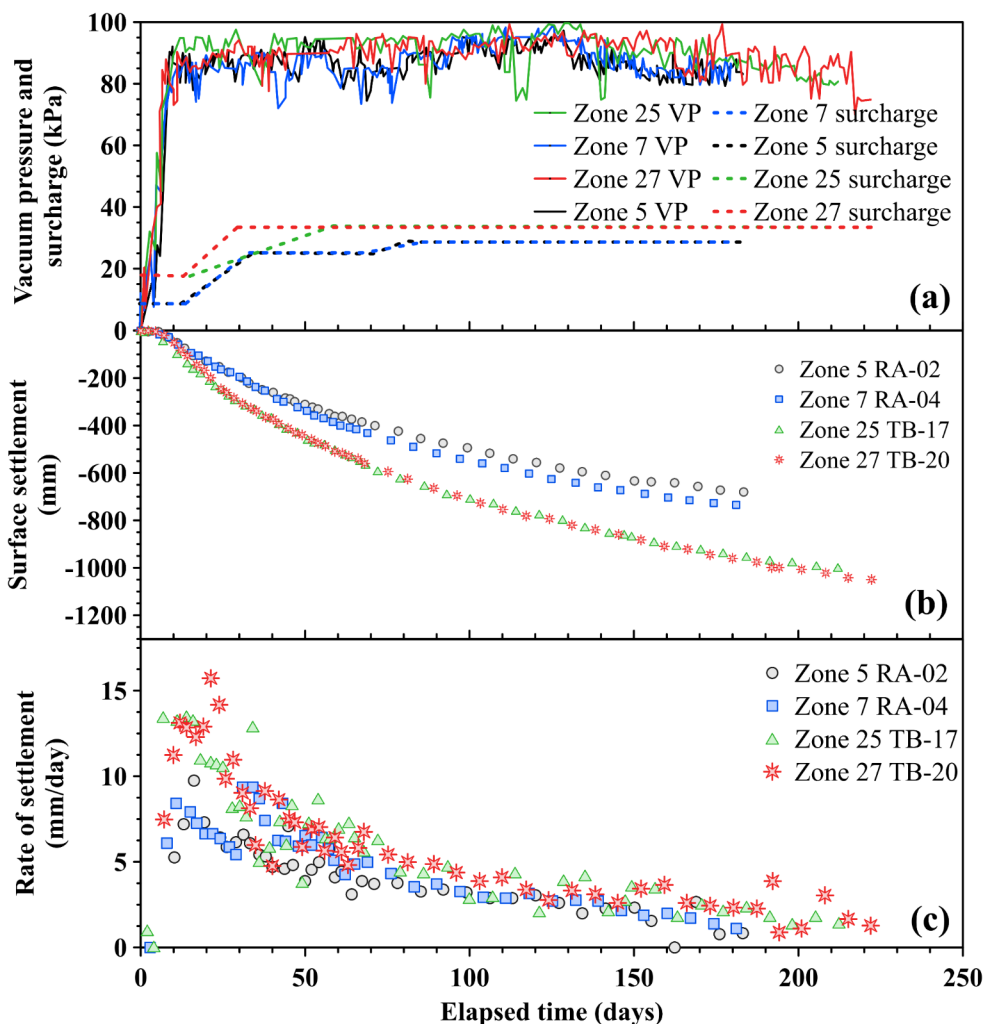


Table 3 Comparison of measured settlement (S_c) and predicted settlement (S_p), degree of consolidation (DOC), and coefficients of consolidation (c_h)

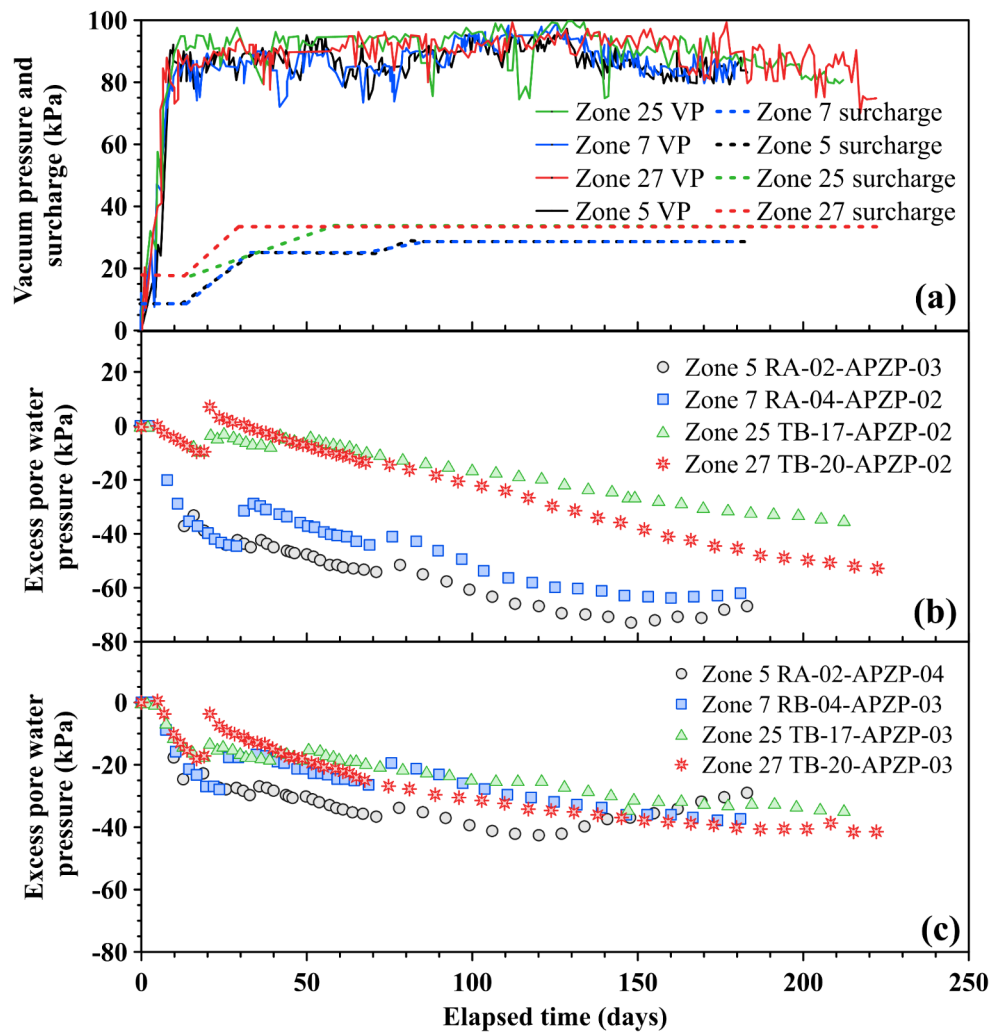
Zone	Observed	Asaoka		Hyperbolic		c_h (m^2/yr)	
	S_c (mm)	S_f (mm)	DOC (%)	S_f (mm)	DOC (%)	$k_v/k_s = 3$	$k_v/k_s = 4$
5	665	731	91	724	92	4.27	5.40
7	731	811	90	806	91	4.41	5.77
25	1002	1112	90	1112	90	3.06	3.87
27	1047	1140	92	1149	91	3.13	3.96

were approximately 30% higher in zones 25 and 27 (previously unimproved soft ground) than in zones 5 and 7 (already been partially improved). The magnitudes of measured settlements are tabulated in Table 3. Furthermore, zones 25 and 27 have higher settlement rates than 5 and 7. However, 90% consolidation was achieved faster in the second improvement areas than in the first improvement areas, implying that the previously installed PVDs in the partially improved zones 5 and 7 regions contributed to their higher permeability.

Pore water pressures with time and depth

Monitoring the excess pore water pressures is essential to verify the effectiveness of the vacuum preloading system applied at the site. Two types of piezometers were used, namely, bored type and push-in type, and were installed at varied depths. The pushed-in type piezometers were installed only at 5 and 10 m depths. The excess pore pressures were obtained by subtracting the piezometer readings from the initial piezometer readings (similar to the dummy

Fig. 10 (a) Vacuum and surcharge, (b) excess pressure at 5 m depth, and (c) excess pressure at 10 m depth versus elapsed time



piezometer readings as shown in Fig. 10. The data of excess pore water pressures with time in zones 5, 7, 25, and 27 can be compared directly. Surprisingly, the zone within the first improvement (with higher settlements) demonstrated less pore pressures than the second improvement zone (with lower settlements) at 5 m depth in the middle of the consolidating clay layer. Moreover, the excess pore pressures were developed faster in the second improvement areas compared to the first improvement areas. The faster development and higher values of excess pore pressures in zones 5 and 7 than the corresponding values in zones 25 and 27 were confirmed, as demonstrated in Fig. 11a and b, respectively. The higher and faster developments of excess pore pressures in zones 5 and 7 showed that the previous partial soft ground improvement using PVDs with conventional surcharge contributed to the higher permeability of the clay layer. Lower values were recorded at 10 m depth, and the bottom of the improved clay layer had similar excess pore pressure readings for zones 5, 7, 25, and 27.

Lateral displacements with time and ground cracks

As mentioned earlier in the field monitoring instrumentation, inclinometers were installed at improved areas in zones 5, 7, 25, and 27. The inward lateral movements towards embankments are plotted in Fig. 12, consisting of lateral movements measured at RA-02 in zone 5, RA-04 in zone 7, TA-15 in zone 25, and TA-18 in zone 27. Larger lateral movements of up to 200 mm were recorded in zones 5 and 7 (second improvement). In comparison, lower lateral movements of up to 60 mm perpendicular to the surcharge embankment were observed in zones 25 and 27 (first improvement) during the preloading stage due to the effects of higher vacuum pressures compared with the embankment surcharge load [15]. A maximum lateral deformation of 500 mm was observed by Chu et al. [5] with a similar loading of -80 kPa vacuum pressure and 2-m-thick surcharge fill. Similar investigations were also performed in other projects [23–25]. The maximum lateral displacement could amount

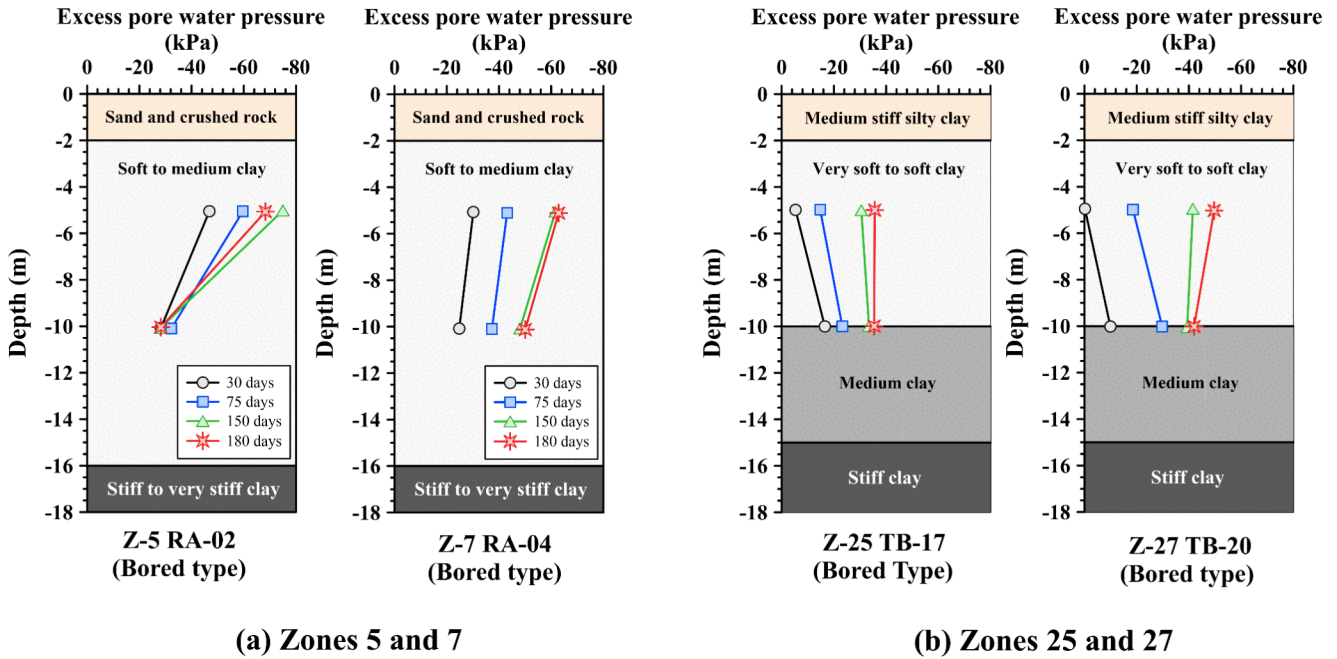


Fig. 11 Excess pore pressure versus depth plots for zones 5, 7, 25, and 27

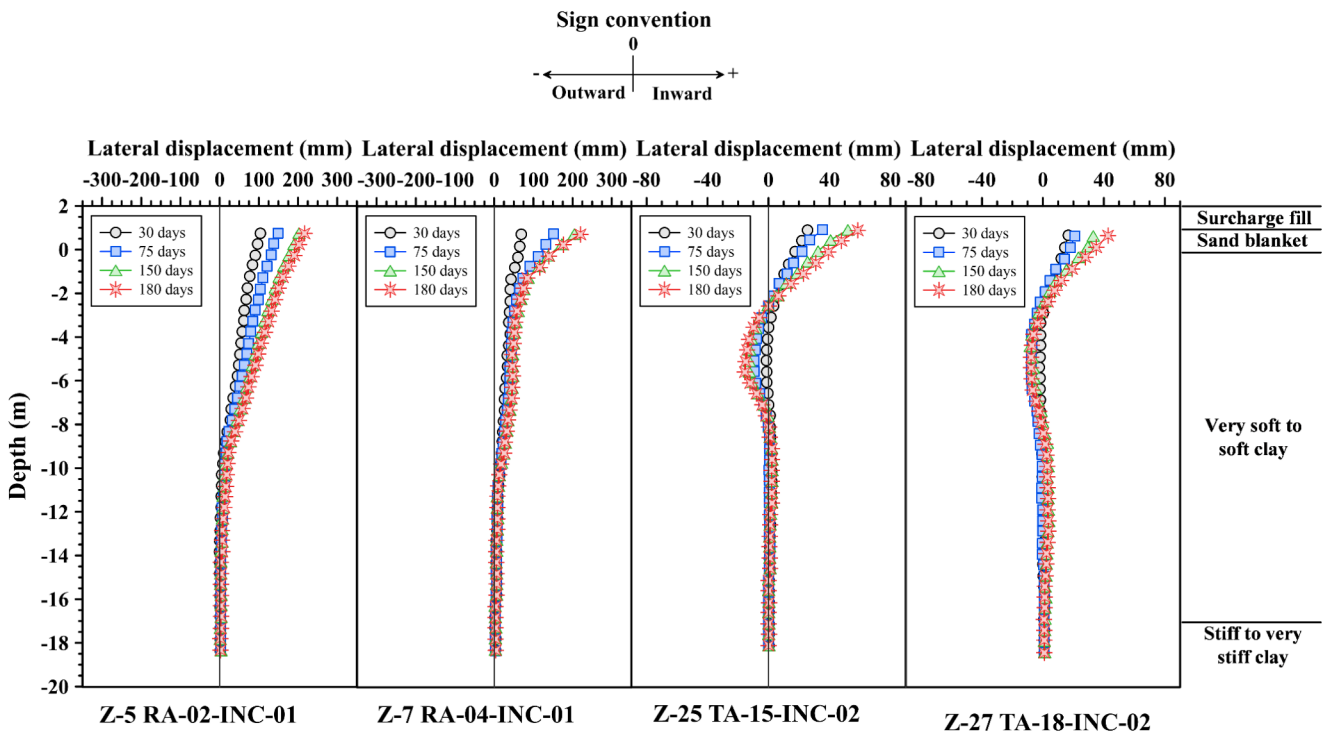


Fig. 12 Lateral displacement profiles with time

to approximately 10% of the vertical settlement observed by other investigators [18, 26–27].

As shown in Fig. 13, the ground cracks were located approximately 6 m from the edge of the trench of the sealing membrane. The ground cracks indicated that vacuum

pressure was greater than the horizontal stresses of soil, causing inward movement. The depth of ground cracks (z_c) could be derived using the groundwater level, shear strength parameters, and active pressures, according to Rankine [28], as follows:



Fig. 13 Ground cracks due to vacuum pressure

$$z_c = \frac{2c'}{\gamma_t \sqrt{K_a}}, \text{ for } z_c < z_w \tag{1}$$

$$z_c = \frac{1}{(\gamma_t - \gamma_w)} \left[\frac{2c'}{\sqrt{K_a}} - \gamma_w z_w \right], \tag{2}$$

for $z_c > z_w$, for $z_c > z$

Where.

z_w	=	groundwater level below the ground surface
γ_t	=	wet unit weight of soil
γ_w	=	unit weight of water
c'	=	effective cohesion of soil
ϕ'	=	friction angle of soil
K_a	=	active earth pressure coefficient = $\tan^2 \left(45 - \frac{\phi'}{2} \right)$

Assuming $c' = 10$ kPa and $\phi' = 23$ degrees, $\gamma_t = 15.8$ kN/m³, and $z_w = 0.5$ m, Eqs. 1 and 2 predicted $z_c = 4.24$ m from the existing ground surface. The depths and locations of cracks could correspond to the monitored lateral movements in Fig. 12.

Predictions of settlements, degrees of consolidation, and back-calculation of c_h values

As tabulated in Table 4, for zones 5 and 7 and 25 and 27, the Asaoka plots [29] to obtain the ultimate settlements are presented in Fig. 14. The ultimate predicted settlements were obtained as 0.731 m, 0.811 m, 1.112 m, and 1.140 m. These predicted ultimate settlements logically agreed with the corresponding observed settlements of 0.665 m, 0.731 m, 1.000 m, and 1.047 m with respective degrees of consolidation (DOC) of 91, 90, 90, and 92%. The first improvement has approximately 30% higher settlements than the second improvement. Also tabulated in Table 4 includes the prediction of ultimate settlements using the hyperbolic method [30] as plotted in Fig. 15 with predicted ultimate settlements of 0.724, 0.806, 1.112, and 1.149 m corresponding to DOCs of 92, 91, 90, and 91% for zones 5, 7, 25 and 27, respectively. The ultimate settlements and DOCs predicted from the Asaoka method generally agreed with the corresponding values predicted by the hyperbolic method.

Following Asaoka's method [29], the c_h values were back-calculated and plotted in Fig. 16 for zones 5, 7, 25,

Table 4 Comparison of measured and predicted settlements, DOCs, and coefficients of consolidation

Zone	Observed	Asaoka		Hyperbolic		c_h (m ² /yr)	
	S_c (mm)	S_f (mm)	DOC (%)	S_f (mm)	DOC (%)	$k_t/k_s = 3$	$k_t/k_s = 4$
5	665	731	91	724	92	4.27	5.40
7	731	811	90	806	91	4.41	5.77
25	1002	1112	90	1112	90	3.06	3.87
27	1047	1140	92	1149	91	3.13	3.96

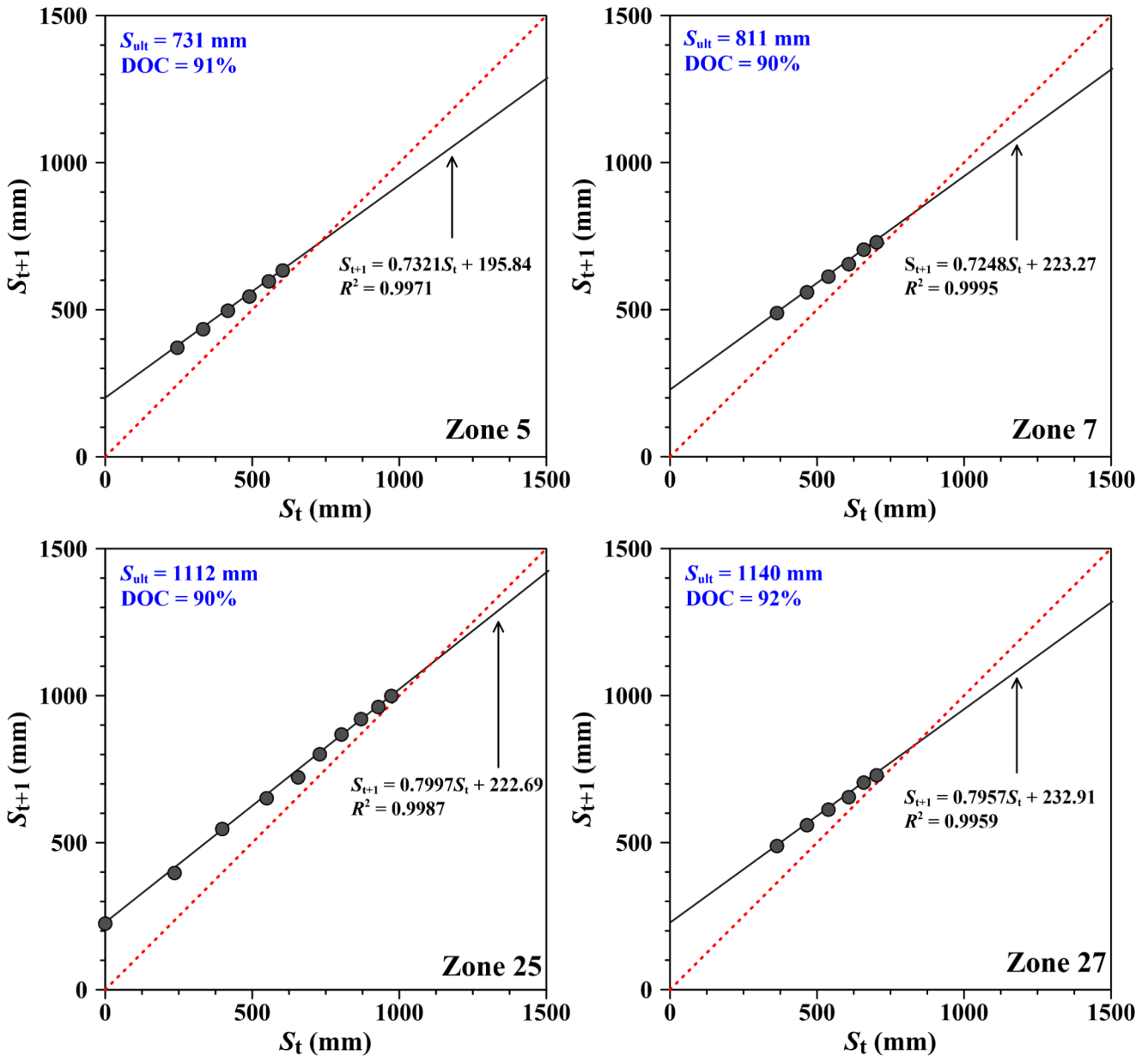


Fig. 14 Prediction of ultimate settlement by Asaoka method

and 27. Previously, Bergado et al. [2, 31] obtained at $d_s/d_m = 2$ and $k_h/k_s = 5$, the average back-calculated value of $c_h = 3\text{ m}^2/\text{yr}$ at the Second Bangkok International Airport using conventional PVD improvement with embankment surcharge. However, previous publications [8–10, 13,14, 22, 32] regarding the improvement of soft Bangkok clay with vacuum-PVD obtained a slight reduction in the k_h/k_s because of increased k_s within the smear zone together with the slight increase of k_h outside the smear zone. Bergado et al. [17] recently reported flocculated microstructures with a high degree of edge-to-face orientation within the smear zone and mixed flocculated and dispersed microstructures

outside. Thus, instead of using $k_h/k_s = 5$ in conventional PVD improvement, as mentioned previously, k_h/k_s of 4 or 3 can be used for Vac-PVD improvement. As also tabulated in Table 4, for $k_h/k_s = 3$, the c_h values of zones 5, 7, 25, and 27 correspond to 4.27, 4.41, 3.06, and 3.13 m^2/yr , as well as for $k_h/k_s = 4$, the c_h values of zones 5, 7, 25 and 27 correspond to 5.4, 5.57, 3.87 and 3.96 m^2/yr . Subsequently, it can be observed that the c_h values at the second improvement (zones 5 and 7) have higher values compared to the c_h values of zones 25 and 27, which can be attributed to the presence of previously installed PVDs during the first partial improvement of zones 5 and 7.

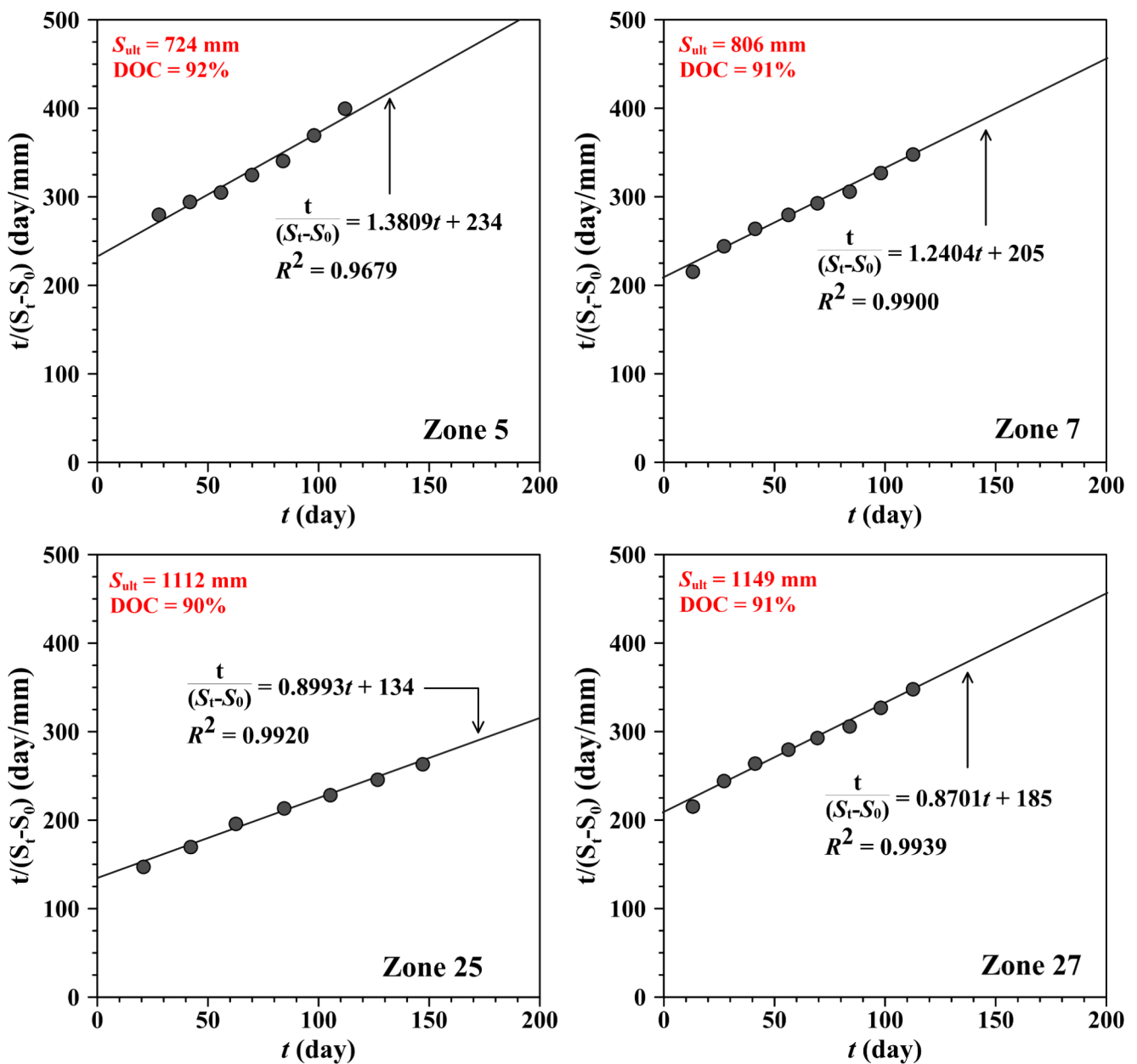


Fig. 15 Prediction of ultimate settlement by hyperbolic method

Comparison of soil properties before and after improvement

As indicated in Fig. 2, two boreholes (BH-1 and BH-2) and one field vane shear test (FVT-1) were done in zones 5 and 7, as well as two boreholes (BH-4 and BH-5) with one field vane test (FVT-1) were performed in zones 25 and 27 after improvement. The undrained vane shear strength increased by twice as much after improvement. As the plasticity of soils increases, undrained shear strength obtained from vane shear tests may give unsafe results for foundation design. For this reason, Bjerrum [33] suggested the

correction factor, a plasticity function. Thus, the field vane shear strengths for this project must be reduced by 20% to obtain the equivalent undrained strengths of the clay. The soil properties from laboratory tests and subsoil investigations after the first and second improvements in zones 5 and 7 are compared in Fig. 17 and tabulated in Table 5 to evaluate the effectiveness of the vacuum-PVD combined with the surcharge embankment method. The index properties, such as the wet unit weights, water contents, and liquid limits, were reduced. The undrained shear strengths increased two times after the first improvement and 1.5 times after the second improvement. The maximum past pressures increased

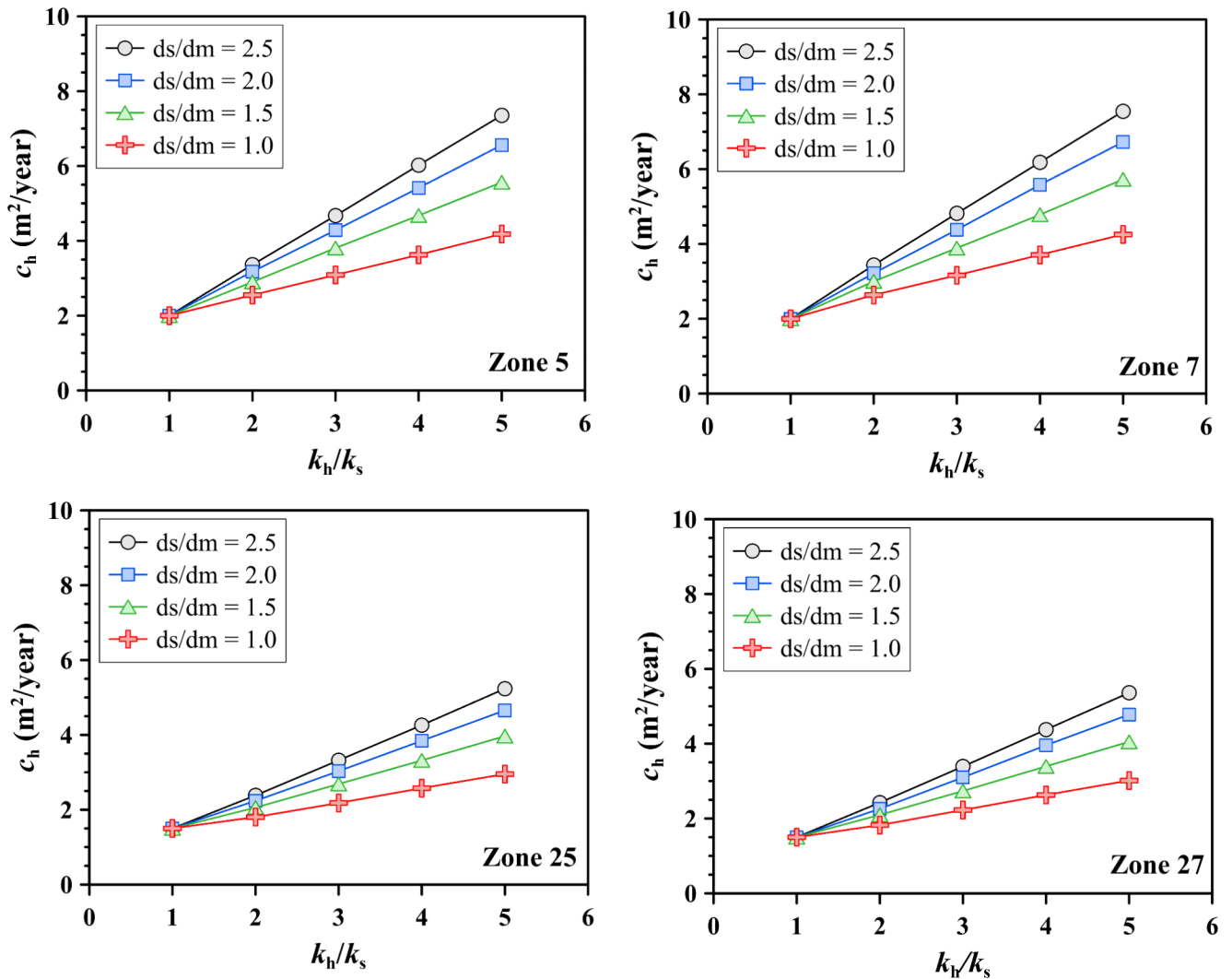


Fig. 16 Back-calculated c_h values using the Asaoka method (After the first improvement)

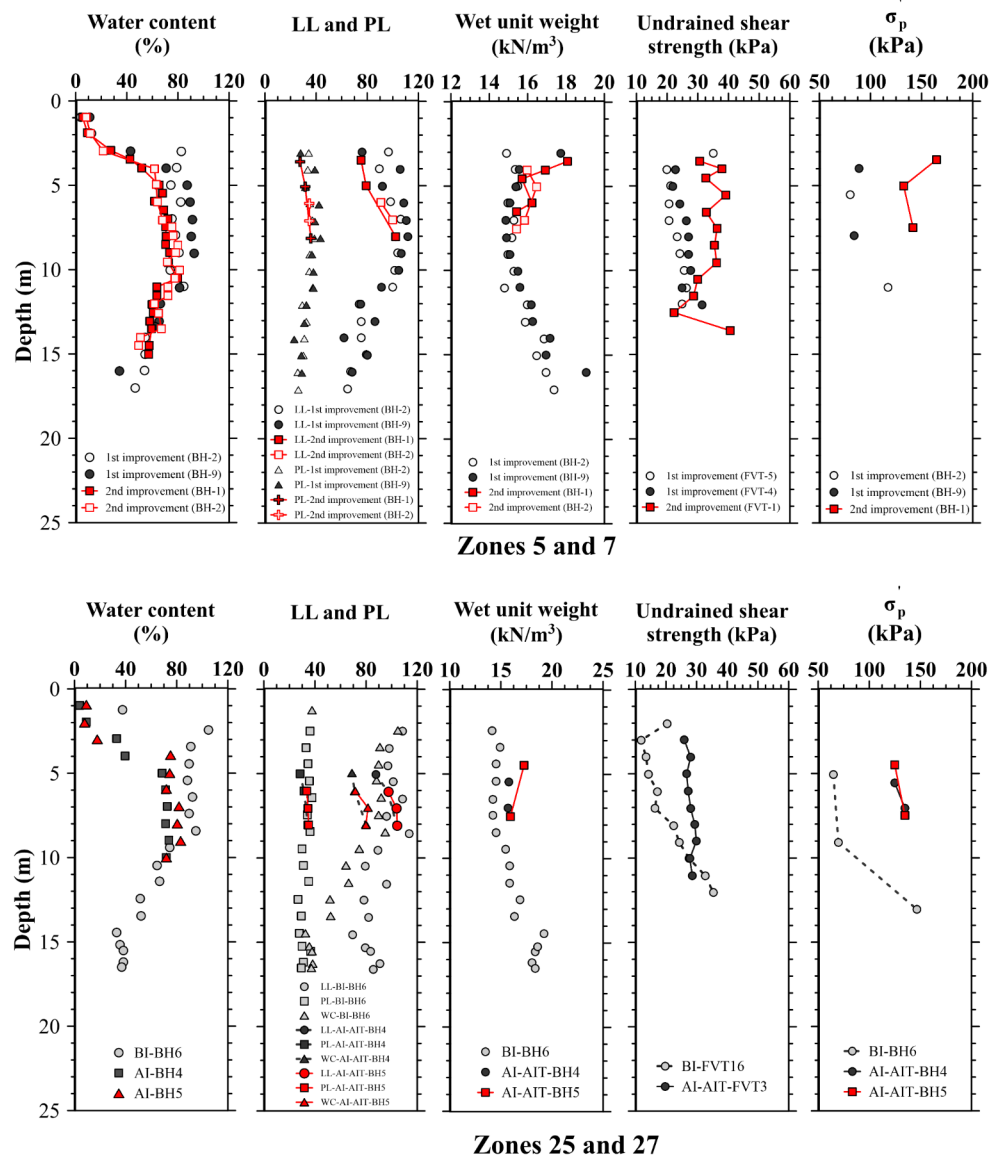
from 60 kPa to 80 kPa after the first partial improvement and 130 kPa after the second improvement. The improved soil properties of the underlying soft ground layer were limited to the lengths of the installed PVDs at 10 m depth.

Similarly, the comparison of soil properties before and after the first improvement in zones 25 and 27 are plotted in Fig. 17 and tabulated in Table 6. As expected, there are reductions in water contents, Atterberg limits, and void ratios with corresponding increases in undrained shear strengths, OCR, and pre-consolidation pressures or maximum past pressures. Most importantly, the maximum past pressures increased almost two times (from 60 to 120 kPa) in the improved uppermost 10 m soft clay layer. Similar observations were obtained from other soft ground improvement projects [2, 18, 22].

Conclusions

The back calculations of monitored data of the second improvement of the third runway extension (North) are compared with the corresponding results of the first improvement of taxiway extension D, including the settlement evolution, pore pressures, and flow parameters. Both sites have been improved using prefabricated vertical drains with vacuum preloading (vacuum-PVD) combined with surcharge, including the field-distributed pumps with air-water separation to maintain efficiency in the vacuum system. The surcharge embankment combined with Vacuum-PVD using an airtight membrane and horizontal prefabricated drain has been successfully applied to improve soft Bangkok clay. Based on the results, the following conclusions can be drawn:

Fig. 17 Comparison of soil properties (before and after improvement) of zones 5, 7, 25, and 27



1. The vacuum-PVD second improvement of previously partially improved soft Bangkok clay using PVD and embankment surcharge at the third runway extension (North) indicated lower settlements as expected, but, in contrast, higher pore pressures and flow parameters (c_h values) were obtained. The previously installed PVDs increased the flow parameters and the evolution of the pore pressures.
2. The first improvement of previously unimproved soft Bangkok clay at the taxiway D extension showed higher settlements as expected. However, lower pore pressures and flow parameters (c_h values) were obtained compared to the improvement in the second runway extension (North).
3. The settlement observations were stopped at a 5 mm/day rate of settlement and 90% degree of consolidation

4. determined by the Asaoka method. The predictions of settlements using the Asaoka method agreed with the corresponding predictions using the hyperbolic method. Lower measured settlements up to 0.7 m were recorded in zones 5 and 7, while higher measured settlements up to 1.0 m were obtained in zones 25 and 27.
4. Combined with the embankment surcharge, the multiple air-water separation sub-tanks in the field that comprised the modified Vacuum-PVD system worked efficiently in generating and maintaining at least -80 kPa to -90 kPa vacuum pressures at the top of the embankment surcharge. The build-up of pore pressures with time was monitored using bored and push-in piezometers. From the readings of the bored-type piezometers in the middle of the soft clay layer (5 m depth), higher pore pressures of up to -60 kPa were generated in zones 5 and 7, while

Table 5 Comparison of soil properties before improvement, after first improvement, and after second improvement for zones 5 and 7

Parameters	Before improvement	After 1st improvement	After 2nd improvement
Soil type	Very soft to soft clay	Soft clay to medium stiff clay	Medium stiff clay
Water content (%)	90–110	71–93	42–82
Liquid limit	90–120	91–109	76–103
Plastic limit	40–45	32–43	28–36
Unit weight (kN/m ³)	15–16	14.6–15.3	15.4–18.11
Compression ratio (CR)	0.20–0.40	0.26–0.35	0.11–0.28
Recompression ratio (RR)	0.02–0.04	0.028–0.034	0.03–0.057
Initial void ratio (e_0)	3–4	2.2–2.5	1.1–2.2
Preconsolidation pressure (kPa)	40–60	77–118	130–164
OCR	1.0–1.5	1.5–3.8	2.1–5.64
s_u (kPa)	8–12	20–30	31–39

Table 6 Comparison of soil properties before and after improvement for zones 25 and 27

Parameters	Before improvement	After improvement
Soil type	Very soft to soft clay	Soft clay to medium stiff clay
Depth (m)	-2.00 to -10.00 m	-3.00 to -10.00 m
Unit weight (kN/m ³)	15–16	15.7–17.3
Water content (%)	75–05	69–82
Liquid limit	90–113	8 – 104
Plastic limit	60–77	27–35
Preconsolidation pressure (kPa)	60–67	125–135
OCR	1.0–1.5	2.8–4.2
Initial void ratio	2.4–2.58	1.90–2.29
CR	0.33–0.37	0.21–0.32
RR	0.042–0.051	0.035–0.061
s_u (kPa)	13–24	26–30

lower pore pressures of up to -50 kPa were recorded in zones 25 and 27.

- Due to vacuum-PVD improvement, the k_h/k_s values were slightly reduced, and the c_h values were increased. The back-calculated c_h values using $d_s/d_m = 2$, and $k_h/k_s = 4$ were higher at 5.40 and 5.57 m²/yr, respectively, for zones 5 and 7. The corresponding values for zones 25 and 27 were lower at 3.87 and 3.96 m²/yr, respectively. The corresponding values from the first improvement using PVD consisted of $d_s/d_m = 2$, $k_h/k_s = 5$, and $c_h = 3$ m²/yr of the previous project involving the adjacent runways at the second Bangkok International Airport. Thus, the k_h/k_s slightly decreased, and c_h increased somewhat.
- After the vacuum-PVD improvement, the very soft to soft clay was transformed into medium-stiff clay. The

index properties, such as the unit weights, water contents, and liquid limits, were reduced. The compression indices and the void ratios were also reduced. The undrained shear strengths increased by twice as much. The maximum past pressures and over-consolidation ratio were increased to more than 120 kPa.

- From inclinometer readings, inward lateral movements were observed up to 200 mm perpendicular to the surcharge embankment due to higher vacuum pressures than the lower embankment surcharge load. Ground cracks were located approximately 6 m from the edge of the trench of the sealing membrane. The ground cracks indicated that vacuum pressure was greater than the horizontal stresses of soil, causing inward movement.

Acknowledgements This research budget was allocated by the National Science, Research, and Innovation Fund (NSRF) and King Mongkut's University of Technology North Bangkok (Project no.KMUTNB-FF-67-A-05). The fourth author (P. Jongpradist) appreciates the financial support provided by the National Research Council of Thailand (NRCT) through Thailand Science Research and Innovation (TSRI) under Fundamental Fund 2025 (Project: Advanced Construction Towards Thailand 4.0). The authors would like to acknowledge Mr. Nuttapon Kovittayanon and Peter Tijnl de Zwart from Ceteau (Thailand) Ltd. for providing the improvement project data and kind cooperation.

Declarations

Ethical approval The authors state that the research was conducted according to ethical standards.

Conflict of interest The authors declare that there is no conflict of interest.

References

- Hansbo S (1979) Consolidation of clay by band-shaped prefabricated drains. *Ground Eng'g* 12(5):16–25
- Bergado DT, Balasubramaniam AS, Fannin RJ, Holtz RD (2002) Prefabricated vertical drains (PVDs) in soft Bangkok clay: a case study of the new Bangkok International Airport project. *Can Geotech J* 39(2):304–315
- Bergado DT, Enriquez AS, Sampaco CL, Alfaro MC, Balasubramaniam AS (1992) Inverse analysis of geotechnical parameters on improved soft Bangkok clay. *J Geotech Eng'g Div ASCE* 118(7):1012–1030
- Kjellmann W (1952) Consolidation of clay soil by means of atmospheric pressure. *Proc on Soil Stabilization Conference, Boston, USA* 1:258–263
- Chu J, Yan SW, Yang H (2000) Soil improvement by the vacuum preloading method for an oil storage station. *Geotechnique* 50(6):625–632
- Chai JC, Ong CY, Carter JP, Bergado DT (2013) Lateral displacement under combined vacuum pressure and embankment loading. *Geotechnique* 63(10):842–856
- Chai JC, Fu HT, Wang J, Shen SL (2020) Behavior of a PVD unit cell under vacuum pressure and a new method for consolidation analysis. *Comput Geotech* 120:103415

8. Saowapakpiboon J, Bergado DT, Thann YM, Voottipruex P (2009) Assessing the performance of PVD with vacuum and heat preloading. *Geosynth Int* 16(5):384–392
9. Saowapakpiboon J, Bergado DT, Youwai S, Chai JC, Wanthong P, Voottipruex P (2010a) Measured and predicted performance of prefabricated vertical drains (PVDs) with and without vacuum preloading. *Geotext Geomembranes* 28(1):1–11
10. Saowapakpiboon J, Bergado DT, Voottipruex P, Lam LG, Nakakuma K (2010b) PVD improvement combined with surcharge and Vacuum Preloading including simulations. *Geotext Geomembr* 29(1):74–82
11. Lam LG, Bergado DT, Hino T (2015) PVD improvement of soft Bangkok clay with and without vacuum preloading using analytical and numerical analyses. *Geotext Geomembranes* 43(6):547–557
12. Long PV, Nguyen LV, Bergado DT, Balasubramaniam AS (2015) Performance of PVD improved soft ground using vacuum consolidation methods with and without airtight membrane. *Geotext Geomembr* 43:473–483
13. Bergado DT, Jamsawang P, Jongpradist P, Likitlersuang S, Pantaeng C, Kovittayanun N, Baez F (2021a) Case study and numerical simulation of PVD improved soft Bangkok clay with surcharge and vacuum preloading using a modified air-water separation system. *Geotext Geomembr* 50(1):137–153
14. Bergado DT, Jamsawang P, Kovittayanun N, Baez F, de Zwart TP (2021b) Vacuum-PVD improvement: a case study of the second improvement of soft Bangkok clay on subsiding ground. *Intl J Geosynthetics Ground Eng* 7:96
15. Chai JC, Carter JP, Hayashi S (2005) Ground deformation induced by vacuum consolidation. *J Geotech Geoenviron Eng* 131(12):1552–1561
16. Chai JC, Carter JP, Hayashi S (2006) Vacuum consolidation and its combination with embankment loading. *Can Geotech J* 43(10):985–996
17. Bergado DT, Chaiyaput S, Artidteang S, Nguyen NT (2020) Microstructures within and outside the smear zone for soft clay improvement using PVD only, Vacuum-PVD, Thermo-PVD and Thermo-Vacuum-PVD. *Geotext Geomembranes* 48(6):828–843
18. Wu J, Xuan Y, Deng Y, Li X, Zha F, Zhou A (2020) Combined vacuum and surcharge preloading method to improve Lianyungang soft marine clay for embankment widening project: a case. *Geotext Geomembranes* 49(2):452–465
19. Deng YF, Liu L, Cui YJ, Feng Q, Chen XL, He N (2018) Colloid effect on clogging mechanism of hydraulic reclamation mud improved by vacuum preloading. *Can Geotech J* 56(5):611–620
20. Xu BH, He N, Jiang YB, Zhou YZ, Zhan XJ (2020) Experimental study on the clogging effect of dredged fill surrounding the PVD under vacuum preloading. *Geotext Geomembranes* 48(5):614–624
21. Cai YQ, Xie ZW, Wang J, Wang P, Geng XY (2018) New approach of vacuum preloading with booster PVDs to improve deep marine strata. *Can Geotech J* 55(10):1359–1371
22. Long PV, Nguyen LV, Tri TD, Balasubramaniam AS (2016) Performance and analyses of thick soft clay deposit improved by PVD with surcharge preloading and vacuum consolidation – a case study at CMIT. *Geotech Eng J SEAGS AGSSEA* 47:1–10
23. Qi C, Li R, Gan F, Zhang W, Han H (2020) Measurement and simulation on consolidation behaviour of soft foundation improved with prefabricated vertical drains. *Int J Geosynth Ground Eng* 6(2):1–10
24. Chu J, Yan SW (2005) Estimation of degree of consolidation for vacuum preloading projects. *Int J Geosynth Ground Eng* 5(2):158–165
25. Wang P, Han Y, Zhou Y (2020) Apparent clogging effect in vacuum-induced consolidation of dredged soil with prefabricated vertical drains (PVDs). *Geotext Geomembr*. <https://doi.org/10.1016/j.geotexmem.2020.02.010>
26. Wang J, Fang ZQ, Cai YQ, Chai JC, Wang P, Geng XY (2018) Preloading using fill surcharge and prefabricated vertical drains for an airport. *Geotext Geomembranes* 46(5):575–585
27. Deng Y, Kan ME, Indraratna B, Zhong R (2017) Finite element analysis of vacuum consolidation with modified compressibility and permeability parameters. *Int J Geosynth Ground Eng* 3(2):1–13
28. Rankine WMJ (1857) On Stability on loose earth. *Philosophic Transactions of Royal Society, London*, pp 9–27
29. Asaoka A (1978) Observational procedure of settlement prediction. *Soils Found* 18(4):87–101
30. Tan TS, Inoue T, Lee SL (1991) Hyperbolic method for consolidation analysis. *J Geotech Geoenviron Eng* 117(1):1723–1737
31. Bergado DT, Long PV, Balasubramaniam AS (1996) Compressibility and flow parameters from PVD improved soft Bangkok clay. *Geotech Eng* 27(1):1–20
32. Artidteang S, Bergado DT, Saowapakpiboon J, Teerachaikulpanich N, Kumar A (2011) Enhancement of efficiency of prefabricated vertical drains using surcharge vacuum and heat preloading. *Geosynthetics Int* 18(1):35–47
33. Bjerrum L (1974) Problems of soil mechanics and construction on soft clays. *Norwegian Geotechnical Institute, Publication No. 110*, Oslo

Publisher's Note Springer Nature remains neutral with regard to jurisdictional claims in published maps and institutional affiliations.

Springer Nature or its licensor (e.g. a society or other partner) holds exclusive rights to this article under a publishing agreement with the author(s) or other rightsholder(s); author self-archiving of the accepted manuscript version of this article is solely governed by the terms of such publishing agreement and applicable law.